ACTA METALLURGICA SLOVACA
2023, VOL. 29, NO. 1, 26-33

RESEARCH PAPER

CRITICAL ANALYSIS OF MATERIAL BEHAVIOUR IN WELDED PLATES OF AISI 0.2%-C STEEL UNDER AS-WELDED, QUENCHED AND ANNEALED CONDITIONS

Saurabh Dewangan[1], *Vedant Vinod Nemade*[1], *Kanad Harshal Nemade*[1*]

[1] Department of Mechanical Engineering, Manipal University Jaipur, Jaipur, Rajasthan, India, Pin-303007

*Corresponding author: kanad.219408006@muj.manipal.edu, Manipal university Jaipur, 303007, Jaipur, Rajasthan, India

Received: 06.02.2023
Accepted: 26.02.2023

ABSTRACT

AISI 1020 grade of steel is well known for its good combination of high strength and fair ductility. Therefore, it is widely demanded in construction sectors. It possesses a good weldability too in both arc and gas welding conditions. In the present work four pairs of AISI 1020-0.2%C steel plates were welded by shielded arc welding method. Except one welded plate, other three were heat treated. Based on the heat treating, three different physical conditions were achieved- water quenched, oil quenched and annealed. All the samples were tested for tensile strength, hardness, and microstructure. The annealed specimen has showed a significantly improved tensile strength of 439 MPa which is 85% higher than as-welded specimen. Water and oil quenched specimens showed lesser strength than that of as-welded specimen. With regard to hardness, there were two different observations. The as-welded and annealed specimens indicated the highest hardness at welded joint whereas the lower values were reported in base metal part. In contrary, the water and oil quenched specimens were harder in base metal zone as compared to welded zone. Both, strength, and hardness were found in good correlation with microstructural appearance of the plates.

Keywords: AISI 1020-0.2% C; Welding; Tension test; Rockwell hardness; Microscopy

INTRODUCTION

AISI 1020 steel, a low carbon grade, is known for its good strength of nearly 420 MPa along with the toughness value of 120 J. In untreated condition, it possesses an average hardness of 123 BHN. This grade of steel is widely used in fabrication and construction works. The weldability of 0.2% steel is very good [1]. Both, autogenous and homogenous type of welding can be performed in 1020 grade. Although the yield parameters during welding greatly affect the joint performance, the post weld heat treatment work can also play an important role to improve the properties to a great extent. Heat treatment, a process of heating, holding and subsequent cooling at desired rate, is not a new technique. It is being utilized from many years [2]. But, a small alteration in process parameters can result into significant variation of mechanical properties. Hence, the old treatment methods are still being utilized with a small variation in peak temperature, soaking period, and cooling media to get the desired output. During welding, a sudden local melting and solidification of metal causes thermal gradient throughout the welded plate. Therefore, a high chance of residual stress formation exists. Mainly, the heat affected zone is influenced by the residual stress. Hence, an adequate heat treatment is adopted to remove all the internal stresses present in the grains of steel.

Annealing, a usually adopted technique, is a process of heating the samples up to austenite range and then cooling them into such a medium which possesses a less thermal conductivity. In this way, a slow cooling rate can result into coarse pearlite formation with improved ductility, toughness and refined strength [3]. In some instances, the samples are hardened by applying various quenching techniques. Quenching does not/partially allow(s) the sample for phase conversion from austenite to pearlite. The final microstructure of quenching comes out as 'martensite' which is highly hard [4].

The present work deals with critical assessment of microstructural changes with three different types of heat treatment. The comparison among annealing, water quenching and oil quenching have been carried out by selecting one sample in as-welded condition.

LITERATURE REVIEW

The post-weld heat treatment has been adopted by many researchers for various grades of steel. Some of the previous outcomes are discussed in this part.

In a work, post weld heat treatment on SAF 2507 steel was performed. The effects of heat treatment were analysed on microstructure and mechanical properties. They found that increment in hardness and reduction in toughness in the welded zone, it was due to the deviation from equilibrium state. They performed a brief heat treatment post-weld. It showed a remarkable increase in the austenite volume fraction in the welded zone. The highest toughness after the post brief heat treatment at 1080 ^{o} C [5]. Järvenpää et al. (2019) studied the effect of reversion-treated and temper-rolled conditions AISI 301LN steel. By autogenous laser welding, coarse columnar grains were produced at the welded zone of 301LN. Also, the HAZ was very narrow in both the conditions, i.e., temper-rolled and reversion-treated. Both structures had weld metal with 240 HV hardness, matching the hot-rolled sheet. The specimens cut across the weld joint had the

same yield strength in reversion-treated and temper-rolled steels, but more than double in hot-rolled steel. Reversion-treated structures had lower but higher elongation than temper-rolled structures. Welded steels had almost the same fatigue life as hot-rolled steel without welding [6]. Jorgea et al. (2018) presented a comparative study among various post-weld heat treatment conditions of HSLA-80 Steel joined by multi-pass welding with coated electrodes. The Charpy impact test indicated that the HAZ was more durable than the welded metal for heat treated samples [7]. The fatigue characteristics of weld metal, fusion line, and fine grain heat affected zone were investigated by taking the surface notch root radii values of 0.1, 0.2, and 0.3 mm. It was seen that fatigue cracks of weld metal and fusion line begun at twin and then propagated along the martensite laths. The fatigue crack in fine grain HAZ propagated through ferrite grains and thereby substantially blocked by fine grain boundaries [8]. Sharma et al. (2018) studied the relation between the heat-treating temperature and holding period of T91 steel (modified 9Cr-1Mo steel), which lead to changes in microstructural properties such as un-tempered and fine martensite, alpha ferrite, fine and coarse precipitates, etc. Hot Wire TIG welding's low heat input reduced the heat affected zone (HAZ). It was found that the soaking time increased the T91 steel's toughness at 760°C due to fine-tempered martensitic formation. The steel specimen soaked for 2h at 760 °C and 790 °C had the most optimal hardness [9]. Pandey et al. (2019) investigated the effect of PWHT on arc welded P92 joint. The experiment involved two different PWHTs. The first one was treated at 760°C for 2 hours and then cooled in air medium. The second sample was treated at 1040°C for 40 mins. The “as welded” sample had a higher degree of microstructural heterogeneity as compared to the PWHT samples. The toughness of the HAZ was lower in case of PWDT and greater in case of PWNT sample than the as-welded sample. In both the PWHTs the heterogeneity gradient reduced along the weld c/s. Ductile fracture was observed in the PWNT sample whereas brittle fracture was observed in the PWDT and as-welded samples. The PWNT sample eliminated the δ ferrite patches, while the PWDT only changed range of hardness of the δ ferrite [10]. PWHT was performed on welded joint of A537CL1 steel and AISI A321 steel. The strength and hardness got reduced by heat treatment. 620 °C temperature was found highly suitable for the least residual stress [11]. Maraging steel and 13-8 Mo stainless steel was joined by TIG. Post-weld ageing significantly improved the yielding, tensile strength, and elongation of the joint [12]. Dua et al. (2019) studied the effect of PWHT on the properties of laser beam joined 2205DSS and Q235 metals. Treatment was done at 600, 700, and 800 °C. At 700 °C, Q235 BM carbon atoms diffused fastest, creating the thickest carbon-depleted layer. Without Fe3C to slow grain boundary migration, the carbon-depleted layer's ferrite grain coarsened quickly. At 600 °C the PWHT was found to be optimal [13]. Due to the abundance of embrittling precipitates and metallurgical changes, joining duplex alloys is difficult, whereas improper welding circumstances and an unbalanced austenite/ferrite phase ratio increase the risk of solidification cracking, corrosion, and decreased ductility. Since thick sections are used in many industries, such as the oil pipeline and shipbuilding industries, where higher productivity is required, this supports the need for higher heat input, interpass temperature optimization, cooling rate optimization, proper consumable selection, and defect-free joints for quick and rapid productivity. To meet the demands for better production without distortion, numerous innovative procedures, such as plasma, laser, PCGTAW, A-TIG, and hybrid welding processes, are being developed, although these cause high ferritization [14]. One of the most efficient ways to stop cracking in laser-welded joints of NiTi/304SS (stainless steel) is to add Ni as filler material. NiTi/Ni/SS joint was heat treated undergo post-weld heat treatment (PWHT) at 650°C and 850°C to enhance its mechanical capabilities. At the welds, more Ni3Ti was seen as the PWHT temperature rose. This process strengthened the sample leading to an increase from 375 HV0.2 to 493 HV0.2 in average hardness and improved the tensile strength. The maximum joint average strength, which is nearly 2.12 times greater than the joint's as-welded strength, was 643 MPa at 850°C PWHT [15]. The viability of dissimilar friction stir welding (FSW) between the Incoloy 825 Ni-based superalloy and the SAF 2507 super duplex stainless steel was assessed. Because of recrystallization and grain refining, the joint showed greater hardness than the base metals. After undergoing tensile testing by SEM, the welded sample demonstrated ductile fracture mode and had equal strength to the Incoloy 825 parent metal [16]. The different stainless steels (AISI304L and AISI430) were welded together using GTAW and then heat treated at temperatures of 860 °C and 960 °C to check the variation in microstructure and mechanical characteristics. The heat-treated plates had achieved the highest tensile strength and a minimal corrosion resistance [17]. Due to inconsistent heating and cooling during welding, residual stresses, deformation, cracking, and HAZ formation might emerge from the operation. V. D. Kalyankar in this publication discuss the effects of different post-weld heat treatments on the characteristics of pressure vessel steels. Numerous issues that arise both during and after welding are discussed, along with details on various heat treatment methodologies that may be used to address these issues. It also contains a summary of the literature study of earlier significant studies upon that and its impact on the mechanical characteristics of the material [18]. In Grade 91 steel, it was seen than corrosion phenomenon was highly active HAZ in the as-welded which further got increased after tempering [19]. Three PWHTs were carried out on laser welded T-250 maraging steel. They are aging (A), solution-aging (SA) and homogenizing+solution+aging (HSA). Finely dispersed Ni3(Ti, Mo) precipitates, tiny martensite laths, and reverted austenite along the grain boundary made up the microstructures of the weld metals produced by the A and SA procedures. This work emphasises how important martensite and the Ni3(Ti, Mo) precipitate are to ensuring the high strength of welded joints. The toughness of welded joints is significantly influenced by the reverted austenite because of its uneven deformation with the martensite matrix. It demonstrates how the removal of reverted austenite during PWHT using the HSA method might affect the mechanical behaviour of welded joints [20]. With variable heat treatment temperatures and times, the microstructure of T91 steel underwent various structural transformations, including the production of untempered martensite, fine martensite, alpha ferrite, fine and coarse precipitates, etc. Due to the Hot Wire TIG welding process's low heat input, the heat affected zone is narrow. With longer soaking times, T91 steel that has been heat treated at 760°C becomes more robust. The production of fine-tempered martensitic is responsible for this. The steel reached its maximum hardness after being immersed for two hours at two different temperatures (760 °C and 790 °C) [21]. The impact of PWHT on grade S690 high strength steel welded connections that have been reheated, quenched, and tempered (RQT) was investigated by M.S. Zhaoa. The hole drilling test reveals that PWHT decreases the residual stress level at that place and tensile results show that it can improve ductility and maximum resistance keeping plastic resistance low. However, it was shown that although the ductility could still be enhanced if the specimens were heated, the drop in load bearing capability was significant [22].

MATERIAL AND METHODS

A total of eight nos. of AISI 1020-0.2% steel plates of dimension 100×50×5 mm were taken in this work. By using shielded metal arc welding, four pairs are joints were made. A common welding

parameter i.e., 50 V voltage and 180 A current was used in each joining. So, the theoretical power input was 9000 W. The electrode, grade E6010, with steel rod of 2 mm and cellulose coated flux was utilized during welding. As the primary aim of this work is to examine the mechanical property alteration via heat treatment, therefore the yield parameters were randomly selected prior to welding. After welding is completed in all four pairs, one plate was kept in as-welded condition while other three were undergone through heat treatment process. These three plates were heated in an induction furnace at 950ºC for 1.5 hr of soaking time. At this stage, the plates became completely red hot. Then, three of them were cooled in three different media like Water, Oil, and Furnace+Sand. The sample got cooled within 0.5 min inside water. This sample was named as 'Water quenched' sample. In case of oil, the sample took nearly 5 min to cool down. This was named as 'Oil quenched' sample. The third sample was cooled in two steps- initial 2 hours in furnace and then cooling inside sand till room temperature. Hence this sample was considered as 'annealed' sample. An outline of experimental work has been shown in **Fig. 1**.

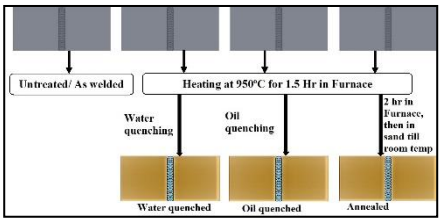

Fig. 1 Outline of the experimental process

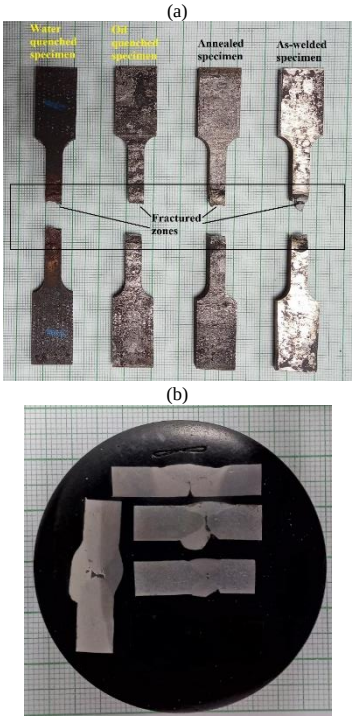

Fig. 2 (a) Fractured tensile test specimens; (b) Polished samples for microstructural analysis

All the four welded plates were cut through wire-electric discharge machining to get tensile test specimens. The specimens were prepared as per ASTM standard. The 10 mm wide plates were cut off from each plate for hardness testing at one cross section and micro-structural testing at another section. Tensile test was performed on a universal testing machine (capacity 600kN). The strain rate was fixed at 0.001 s^{-1}. The stress-strain graphs were plotted during each tensile test. Fractured tension test specimens are shown in **Fig. 2** (a). For hardness testing, Rockwell hardness (B-scale) test was conducted on the cross-sectional surfaces of each welded plate. A total of 31 indentation were done on each plate in such a way that one indent was done in the centre of welded joint, 15 indents were on the left side of the plate and another 15 indents on the right side. There was a gap of 2 mm maintained between each indent. For microstructural study, the plates were superfinished by using a rotating disc polishing machine. The plates were first inserted in a hard-rubber mould and then polished together. Various grades of sandpapers, i.e., of grit sizes 1000, 1400, 1800, 2200, 3000 were utilized for polishing the samples. Nital etchant was prepared and applied on the polished surfaces of the plates before microscopic observation. The polished samples are shown in **Fig. 2** (b).

RESULTS AND DISCUSSION

The experiment-wise results have been discussed in this section.

Tensile test analysis: The stress-strain graphs of as-welded, water quenched, oil quenched and annealed specimen have been provided in **Fig. 3**. The *as-welded* sample had shown the ultimate tensile strength (UTS) of 237 MPa. The maximum strain reported in the sample was 6.1%. An approximate value of yield strength of the sample was 75 MPa. The outcomes of as-welded samples were kept as reference for other samples. In general, the attributes of as-welded sample are ductile because of possessing fair development of elongation prior to fracture. The *water-quenched* sample had shown a UTS of 208 MPa which is nearly 12% lower than that of as-welded sample. Also, there is a great reduction in elongation prior to failure. The strain in this sample was observed as 3.6% only which is 41% smaller than that of as-welded sample. Water quenched sample, being rapidly cooled, did not get sufficient time to change its phase from austenite to pearlite. Therefore, a brittle martensitic structure had reduced its strength and ductility to a great extent. *Oil-quenched* sample showed a bit improvement in tensile properties as compared with water quenched sample. The UTS value and strain of oil-quenched sample were reported as 227 MPa and 5.5% respectively. The UTS of oil quenched sample is almost 4% lower than as-welded specimen whereas its value is 9% higher than water quenched product. Also, the strain recorded in oil quenched

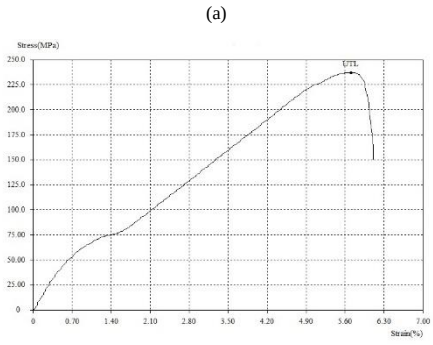

(b)

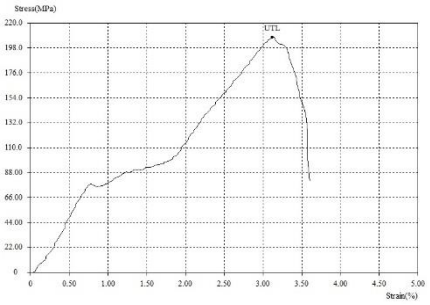

(c)

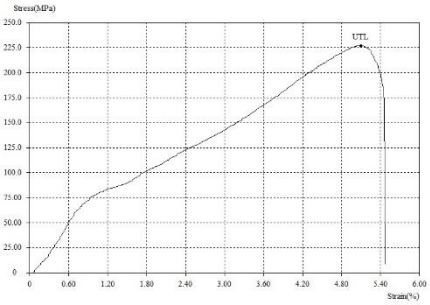

(d)

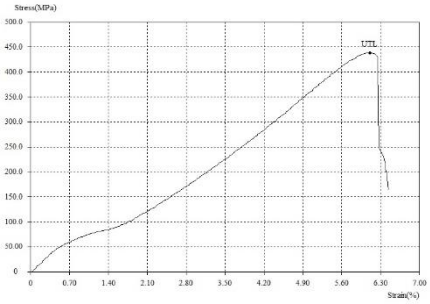

Fig. 3 Stress-strain graph of (a) As-welded sample; (b) Water quenched sample; (c) Oil quenched sample; (d) Annealed sample

sample has got improved by 52% with respect to water quenched sample, although this value is still 10% lesser than as-welded sample. *Annealed* sample was provided sufficient time to get cooled up to room temperature. It showed the UTS of 439 MPa which nearly 85% higher than as -welded product. With such an improved strength, the elongation shown by the sample is also very high (7% higher).

Fractography analysis: The fractured samples from tensile testing have been utilized for field emission scanning electron microscopy (FESEM). The central part of the fractured zone was focussed and observed under high magnification value of 1500 X. The images in all the samples were recorded at a same scale of 10 μm. The objective behind this study is to evaluate the nature of failure- brittle and/or ductile. The symptoms observed in as-welded sample are numerous dimples, micro-pores and macro-pores (**Fig. 4a**). Also, some indications of plastic flow of metal could be noted in this. These all are highly related with ductile failure and therefore this sample showed a good elongation prior to fracture. The FESEM image of water-quenched sample is shown in Fig. 4(b). Dimples are available in this image. Unlike, as welded sample, pores and whirl-like plastic flow of metal are completely absent. It means that water quenching has made the metal some brittle as compared with as-welded one. The fractography image of oil-quenched sample is shown in Fig. 4(c) in which, similar to water-quenched, dimples are present with no substantial pores. In addition, little zones of plastically deformed zones were also reported in the same. Both the indications, i.e., ductile and brittle fracture were observed in the oil-quenched sample. Fig. 4(d) is representing the FESEM image of annealed sample. This image is full of whirl-like appearance which is nothing but plastic flow of material under the effect of tensile loading. Pores are the central part of these whirls. Numerous micro-dimples are present all over the fractured surface. These symptoms are mainly belong to ductile behaviour of the material.

(a)

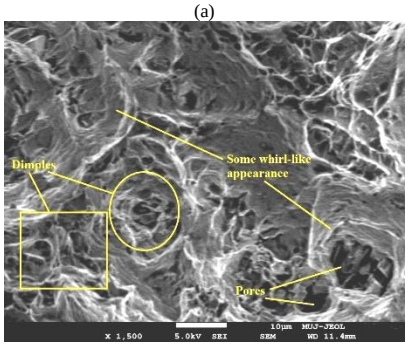

(b)

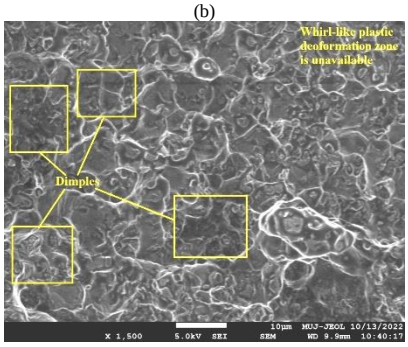

(c)

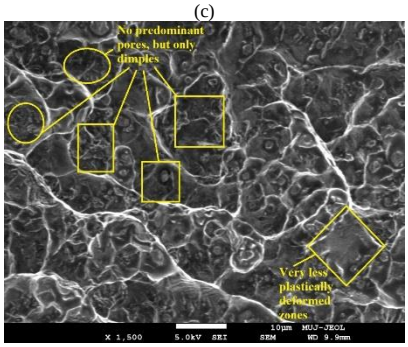

(d)

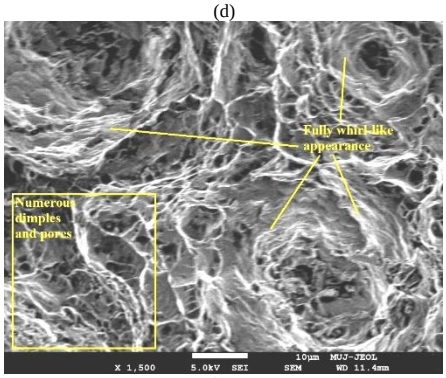

Fig. 4 Fractography analysis of broken tensile specimens; (a) as-welded; (b) Water quenched; (c) Oil quenched; (d) Annealed

Hardness analysis: Rockwell hardness (B scale) tests were performed on the cross-sectional surfaces of four welded plates. The surfaces were made smooth prior to test. Total 31 indents were made on each plate out of which one was made on the centre-position of the plate, i.e., in welded zone. 15 indents were made on left side of the plates, and another 15 sets were on right side also. Based on the recorded hardness values, a comparative graph has been plotted (**Fig. 5**). The hardness profile of water quenched and oil quenched samples are similar in nature. Too, the pattern of graphs in as-welded and annealed samples are alike. Hardness at base metal zone is higher than welded zone in both water & oil quenched specimens whereas the welded zone was found harder than BM in annealed and as-welded specimens. The average values of hardness at BM, HAZ and WZ in as-welded specimen are 69 HRB, 71 HRB, and 73.2 HRB respectively. The water quenched specimen has shown an increment of hardness by 14%, 5%, and 5% at BM, HAZ and WZ respectively in comparison to as-welded specimen. In a similar manner to water quenched sample, oil quenched product has shown almost same increment in hardness. Annealing has reduced, but not significantly, the hardness at all the zones. The reduction percentage at BM, HAZ, and WZ is 4%, 6%, and 7% respectively. A comparative bar chart of hardness in correlation with microscopic views at BM, HAZ and WZ is shown in **Fig. 6**.

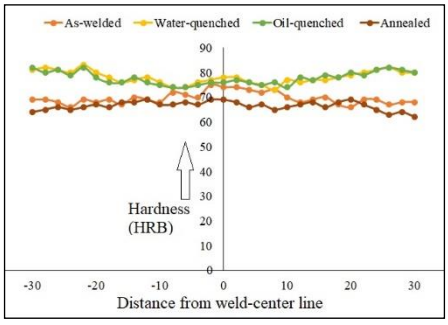

Fig. 5 Hardness profile of four different welded plates

Microstructural analysis: The microstructural appearance at three different zones is completely different in all the four welded plates. The heat treatment has completely varied the grain structure of the same. **Fig. 7** is showing the microstructure of as-welded specimen in three different zones. The BM consists of mainly ferrite and pearlite. Ferrite is predominantly available in the same whereas the appearance of pearlite is relatively fine. The ferrite can be recognized by its bright coloured appearance while pearlite is completely black (Fig. 7a). The fusion boundary can be seen in Fig. 7(b). The equiaxed ferrite has started to elongate from this zone. Also, a high amount of pearlite transformation has begun. Fig. 7(c) is focussed on welded zone where both coarse and fine pearlite can be seen. The ferrite and pearlite lamella are elongated in this zone.

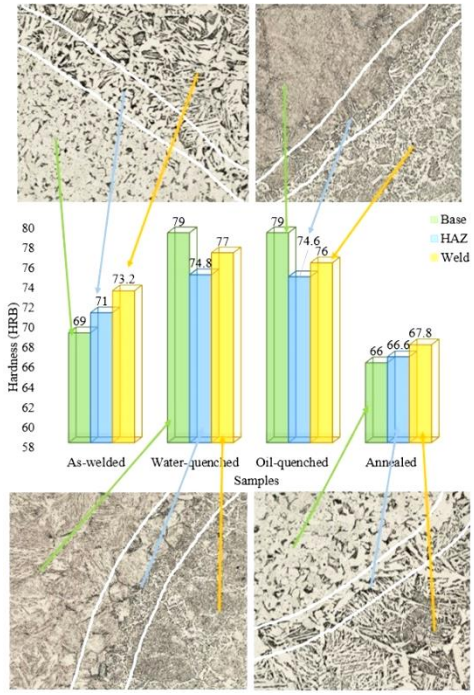

Fig. 6 Comparative analysis of hardness at various zones of the plate

Fig. 8 belongs to the microstructure of water quenched plate. The BM is fully containing acicular martensite. Pearlite is almost negligible in this region. A clear view of needle shaped martensite is shown in Fig. 8(a) inside white rectangles. In fig. 8(b), a transition between BM and WZ can be seen where the martensite has started to convert into pearlite. Pearlitic growth could be seen in boundaries. Fig. 8(c) is the welded zone where a little amount of martensite is still existing, but the major part is composed of both fine and coarse pearlite. Some lamellar α+Fe_3C could also be reported in this zone. Due to this structure, the WZ in water quenched specimen has become less hard than BM.

Fig. 9 shows the microscopic images of oil quenched sample. Unlike water quenched sample, the BM imparts martensite as well as pearlite. As oil has provided a little lesser cooling rate than water, some amount of austenite has converted into pearlite also. As soon as the study shifts towards WZ, a transition from martensitic structure to pearlitic structure can be seen. The fusion boundary consists elongated ferrite and very fine pearlite (Fig. 9b). The WZ is fully composed of very fine pearlite, few martensite and a very little amount of coarse pearlite. All the structures have been properly indicated in the figure itself.

The annealed sample showed a coarse and equiaxed ferrite contents in the BM zone (**Fig. 10a**). The appearance of pearlite (black) is relatively coarser also. It is because of very slow cooling rate. A sufficient time has been provided to sample to convert into fully ferrite and pearlite. At the fusion boundary (Fig. 10b), the equiaxed α+Fe_3C has started to transform into elongated ferrite and pearlite. In the WZ (Fig. 10c), both fine and coarse pearlite have been reported. A columnar growth of ferrite with Fe_3C boundaries have been observed. Some dendrites of ferrite could also be observed in the WZ. Due to this structure tensile strength of the samples got increased with a loss of hardness.

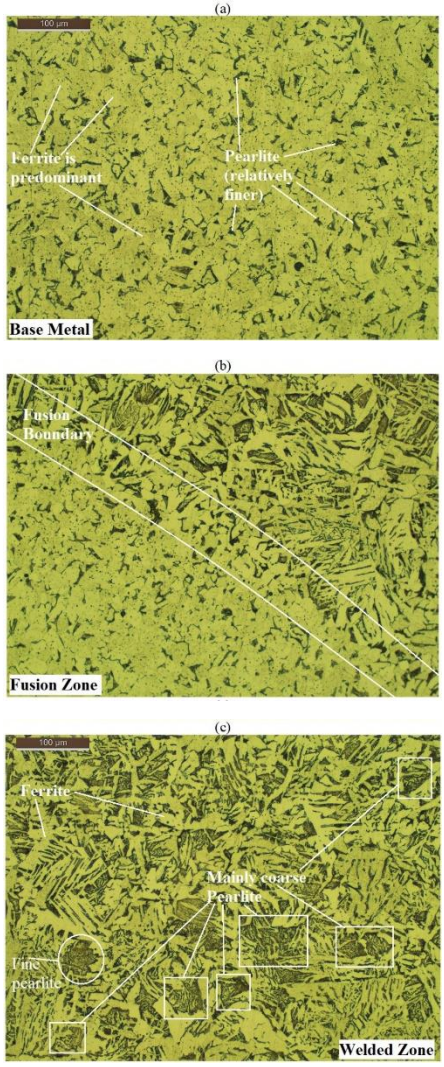

Fig. 7 Microstructure of as-welded specimen; (a) at BM; (b) at HAZ; (c) at WZ

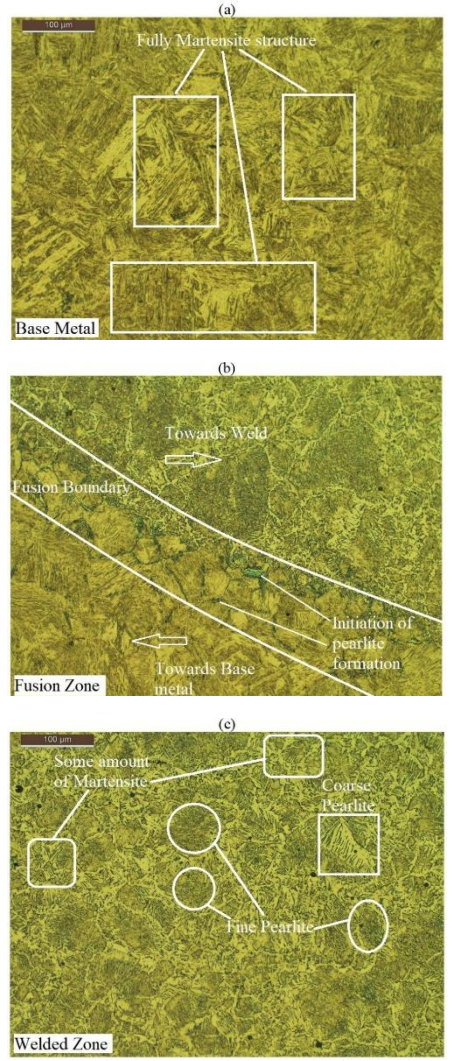

Fig. 8 Microstructure of water-quenched specimen; (a) at BM; (b) at HAZ; (c) at WZ

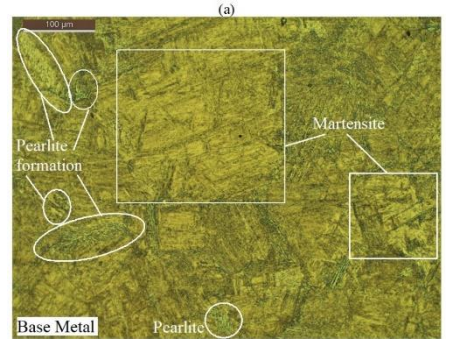

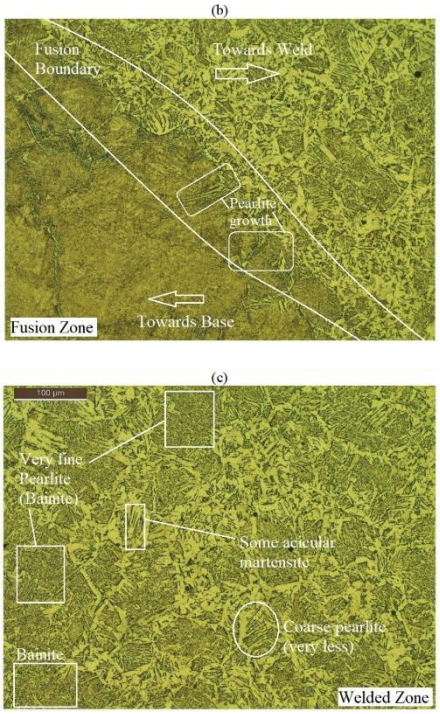

Fig. 9 Microstructure of oil-quenched specimen; (a) at BM; (b) at HAZ; (c) at WZ

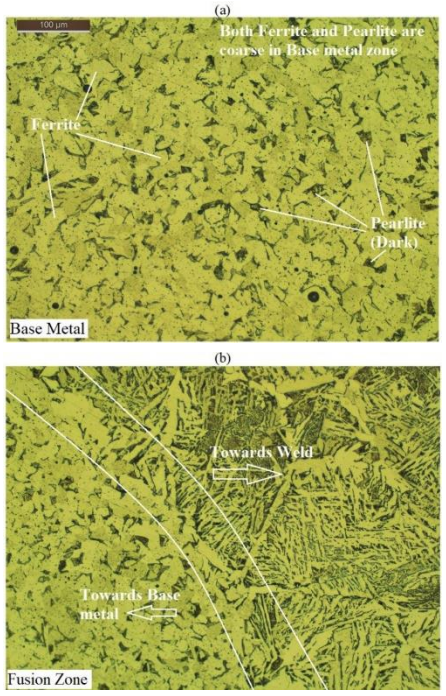

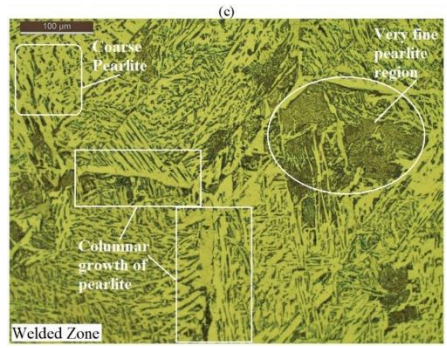

Fig. 10 Microstructure of annealed specimen; (a) at BM; (b) at HAZ; (c) at WZ

DISCUSSION AND CONCLUSION

The present work represents a comparative assessment of water quenched, oil quenched and annealed and un-treated welded specimens of AISI 1020-0.2%C steel on the basis of tensile strength, hardness and critical microstructural observations. Heat treatment has significantly modified the mechanical characteristics of the plates. The observations can be concluded as follows:

- As per the tensile test results, it was seen that both types of quenching have negative effects on strength. All the samples got broken through the welded joint. Water and oil media has reduced the tensile strength of the plates by 12% and 4% respectively, although oil quenched product has provided a comparable value of strength with as-welded plate. The annealed specimen has shown a great improvement in strength i.e., 85% higher than as-welded plate.
- The elongation provided by the samples during tensile tests is completely different in each condition. Water and oil quenched specimens showed lesser values of strain i.e., 41% and 5.5% lesser than as-welded. Annealed sample has attained high ductility and hence its strain value was recorded as 6.5%. These results have been established by the fractography analysis. Both as-welded and annealed samples exhibit plastically deformed zone along with numerous dimples whereas the quenched specimens have no symptoms of any plastic flow.
- Based on hardness results, it was observed than both the quenching media have improved the hardness of BM and reduced the same for WZ. The hardness profile of as-welded and annealed specimens is almost same. In these two, WZ has been reported harder than BM and HAZ.
- Microstructural appearance of four different plates corroborate with the mechanical properties of them. Possessing martensitic structure at the BM zone, both the quenched specimens are hard. At welded joint, martensite has substantially changed into pearlite. In case of annealed sample, the coarse and equiaxed $\alpha+Fe_3C$ at BM has got elongated in the form of dendrites at WZ.

REFERENCES

1. S. Dewangan, N. Mainwal, M. Khandelwal, P.S. Jadhav. Performance analysis of heat treated AISI 1020 steel samples on the basis of various destructive mechanical testing and microstructural behaviour. Australian Journal of Mechanical Engineering, 20:1, 2022, 74-87.

https://doi.org/10.1080/14484846.2019.1664212
2. S. Dewangan, S. K. Selvaraj, B. Karthikeyan, T. M. Adane, S. Chattopadhyaya, G. Krolczyk, R. Raju. Metallographic Investigation on Postweld Heat-Treated 0.21%C-1020 Steel Plates Joined by SMAW Method. Advances in Materials Science and Engineering Volume 2022, Article ID 9377591, 11 pages. https://doi.org/10.1155/2022/9377591
3. Black J T and Kohser R A 2008 DeGarmo's Materials and Processes in Manufacturing (New York: Wiley) 10th edn
4. W. D. Callister, D. G. Rethwisch: Materials Science and Engineering: An Introduction, 10th Edition, John Wiley and Sons, New York, 2018. ISBN: 978-1-119-40549-8
5. Z. Zhang, H. Zhang, J. Hu, X. Qi, Y. Bian, A. Shen, P. Xu, Y. Zhao. Microstructure evolution and mechanical properties of briefly heat treated SAF 2507 super duplex stainless steel welds. Construction and Building Materials 168 (2018) 338–345. https://doi.org/10.1016/j.conbuildmat.2018.02.143
6. A. Järvenpää, M. Jaskari, M. Keskitalo, K. Mäntyjärvi, P. Karjalainen. Microstructure and mechanical properties of laser-welded high- strength AISI 301LN steel in reversion-treated and temper-rolled conditions. Procedia Manufacturing 36 (2019) 216–223. https://doi.org/10.1016/j.promfg.2019.08.028
7. L. J. Jorge, V. S. Cândido, A. C. R. Silva, F. C. G. Filho, A. C. Pereira, F. S. Luz, S. N. Monteiro. Mechanical properties and microstructure of SMAW welded and thermically treated HSLA-80 steel. https://doi.org/10.1016/j.jmrt.2018.08.007
8. N. Yamaguchi, G. Lemoine, T. Shiozaki, Y. Tamai. Effect of microstructures on notch fatigue properties in ultra-high strength steel sheet welded joint. International Journal of Fatigue 129 (2019) 105233. https://doi.org/10.1016/j.ijfatigue.2019.105233
9. A. Sharma, D. Kant Verma, S. Kumaran. Effect of post weld heat treatment on microstructure and mechanical properties of Hot Wire GTA welded joints of SA213 T91 steel. Materials Today: Proceedings 5 (2018) 8049–8056. https://doi.org/10.1016/j.matpr.2017.11.490
10. C. Pandey, M. M. Mahapatra, P. Kumar, J. G. Thakre, N. Saini. Role of evolving microstructure on the mechanical behaviour of P92 steel T welded joint in as-welded and post weld heat treated state. Journal of Materials Processing Tech. 263 (2019) 241–255. https://doi.org/10.1016/j.jmatprotec.2018.08.032
11. B. Sadeghia, H. Sharifi, M. Rafiei, M. Tayebi. Effects of post weld heat treatment on residual stress and mechanical properties of GTAW: The case of joining A537CL1 pressure vessel steel and A321 austenitic stainless steel. Engineering Failure Analysis 94 (2018) 396–406. https://doi.org/10.1016/j.engfailanal.2018.08.007
12. C.V.S. Murthy, A. Gopala Krishna, G.M. Reddy. Microstructure and mechanical properties of similar and dissimilar metal gas tungsten constricted arc welds: Maraging steel to 13-8 Mo stainless steel. Defence Technology. https://doi.org/10.1016/j.dt.2018.04.005.
13. C. Dua, X. Wanga, C. Luo. Effect of post-weld heat treatment on the microstructure and mechanical properties of the 2205DSS/Q235 laser beam welding joint. Journal of Materials Processing Tech. 263 (2019) 138–150. https://doi.org/10.1016/j.jmatprotec.2018.08.013
14. J. Verma, R. V. Taiwade. Effect of welding processes and conditions on the microstructure, mechanical properties and corrosion resistance of duplex stainless-steel weldments—A review. Journal of Manufacturing Processes 25(2017)134–152. https://doi.org/10.1016/j.jmapro.2016.11.003
15. Y. Chen, S. Sun, T. Zhang, X. Zhou, S. Li. Effects of post-weld heat treatment on the microstructure and mechanical properties of laser-welded NiTi/304SS joint with Ni filler. Materials Science & Engineering A. https://doi.org/10.1016/j.msea.2019.138545
16. J. Kangazian, M. Shamanian. Microstructure and mechanical characterization of Incoloy 825 Ni-based alloy welded to 2507 super duplex stainless steel through dissimilar friction stir welding. Trans. Nonferrous Met. Soc. China 29(2019) 1677−1688. https://doi.org/10.1016/S1003-6326(19)65074-0
17. S. Ghorbani, R. Ghasemi, R. Ebrahimi-Kahrizsangi, A. H. Najafabadi. Effect of post weld heat treatment (PWHT) on the microstructure,mechanical properties, and corrosion resistance of dissimilar stainless steels. Materials Science & Engineering A 688 (2017) 470–479. https://doi.org/10.1016/j.msea.2017.02.020
18. V. D. Kalyankar, Gautam Chudasam. Effect of post weld heat treatment on mechanical properties of pressure vessel steels. Materials Today: Proceedings 5 (2018) 24675–24684. https://doi.org/10.1016/j.matpr.2018.10.265
19. A. Lanzutti, F. Andreatta, M. Lekka, L. Fedrizzi. Microstructural and local electrochemical characterisation of Gr. 91 steel-welded joints as function of post-weld heat treatments. Corrosion Science 148 (2019) 407–417. https://doi.org/10.1016/j.corsci.2018.12.042
20. K. Li, J. Shan, C. Wang, Z. Tian. Effect of post-weld heat treatments on strength and toughness behavior of T-250 maraging steel welded by laser beam. Materials Science & Engineering A 663 (2016) 157–165. https://doi.org/10.1016/j.msea.2016.03.082
21. A. Sharma, D. K. Verma, S. Kumaran. Effect of post weld heat treatment on microstructure and mechanical properties of Hot Wire GTA welded joints of SA213 T91 steel. Materials Today: Proceedings 5 (2018) 8049–8056. https://doi.org/10.1016/j.matpr.2017.11.490
22. M.S. Zhao, S.P.Chiew, C.K. Lee. Post weld heat treatment for high strength steel welded connections. Journal of Constructional Steel Research 122 (2016) 167–177. https://doi.org/10.1016/j.jcsr.2016.03.015